Dynamic wetting and spreading and the role of topography

2009 J. Phys.: Condens. Matter 21 464122

(http://iopscience.iop.org/0953-8984/21/46/464122)

J. Phys.: Condens. Matter **21** (2009) 464122 (11pp) doi:10.1088/0953-8984/21/46/464122

Dynamic wetting and spreading and the role of topography

Glen McHale[1], **Michael I Newton and Neil J Shirtcliffe**

School of Science and Technology, Nottingham Trent University, Clifton Lane, Nottingham NG11 8NS, UK

E-mail: glen.mchale@ntu.ac.uk

Received 4 April 2009, in final form 30 May 2009
Published 29 October 2009
Online at stacks.iop.org/JPhysCM/21/464122

Abstract

The spreading of a droplet of a liquid on a smooth solid surface is often described by the Hoffman–de Gennes law, which relates the edge speed, v_e, to the dynamic and equilibrium contact angles θ and θ_e through $v_e \propto \theta(\theta^2 - \theta_e^2)$. When the liquid wets the surface completely and the equilibrium contact angle vanishes, the edge speed is proportional to the cube of the dynamic contact angle. When the droplets are non-volatile this law gives rise to simple power laws with time for the contact angle and other parameters in both the capillary and gravity dominated regimes. On a textured surface, the equilibrium state of a droplet is strongly modified due to the amplification of the surface chemistry induced tendencies by the topography. The most common example is the conversion of hydrophobicity into superhydrophobicity. However, when the surface chemistry favors partial wetting, topography can result in a droplet spreading completely. A further, frequently overlooked consequence of topography is that the rate at which an out-of-equilibrium droplet spreads should also be modified. In this report, we review ideas related to the idea of topography induced wetting and consider how this may relate to dynamic wetting and the rate of droplet spreading. We consider the effect of the Wenzel and Cassie–Baxter equations on the driving forces and discuss how these may modify power laws for spreading. We relate the ideas to both the hydrodynamic viscous dissipation model and the molecular-kinetic theory of spreading. This suggests roughness and solid surface fraction modified Hoffman–de Gennes laws relating the edge speed to the dynamic and equilibrium contact angle. We also consider the spreading of small droplets and stripes of non-volatile liquids in the capillary regime and large droplets in the gravity regime. In the case of small non-volatile droplets spreading completely, a roughness modified Tanner's law giving the dependence of dynamic contact angle on time is presented. We review existing data for the spreading of small droplets of polydimethylsiloxane oil on surfaces decorated with micro-posts. On these surfaces, the initial droplet spreads with an approximately constant volume and the edge speed–dynamic contact angle relationship follows a power law $v_e \propto \theta^p$. As the surface texture becomes stronger the exponent goes from $p = 3$ towards $p = 1$ in agreement with a Wenzel roughness driven spreading and a roughness modified Hoffman–de Gennes power law. Finally, we suggest that when a droplet spreads to a final partial wetting state on a rough surface, it approaches its Wenzel equilibrium contact angle in an exponential manner with a time constant dependent on roughness.

1. Introduction

A droplet deposited onto a solid substrate will rapidly adopt a shape determined by the forces due to surface tension and gravity. At equilibrium at the contact line it will also locally obey Young's law, $\cos\theta_e = (\gamma_{SV} - \gamma_{SL})/\gamma_{LV}$, where θ_e is the equilibrium contact angle and the γ_{ij} are the interfacial tensions between the solid, liquid and vapor interfaces [1, 2]. However, when first deposited, a droplet is far from equilibrium and so the contact angle has a dynamic value θ, which evolves with time, t. On a smooth and flat surface the characteristic speed at which this evolution occurs is given

[1] Author to whom any correspondence should be addressed.

by $v^* = \gamma_{LV}/\eta$ where η is the viscosity of the liquid; this suggests defining a non-dimensional capillary number $Ca = v_e/v^*$. Indeed, from studies of silicone oils displacing air in glass capillaries Hoffman had suggested that for complete wetting systems with $\theta_e = 0°$ the dynamic contact angle was a universal function of the capillary number [3, 4] and Voinov had shown that $\theta \propto Ca^{1/3}$ could fit the low velocity data [5]. In the case of a small droplet of characteristic size less than the capillary length, $\kappa^{-1} = (\gamma_{LV}/\rho g)^{1/2}$ where ρ is the density of the liquid and $g = 9.81$ m s^{-2} is the acceleration due to gravity, the associated characteristic time for spreading is $\tau^* = \kappa^{-1}/v^*$. A simple view of spreading of a small droplet is that the driving force per unit length of contact line is given by the out-of-balance surface tension and gravity forces described by $\gamma_{LV}(\cos\theta_e - \cos\theta)$, and the spreading is resisted by viscous forces $\propto \eta v_e/\theta$ [6]. This hydrodynamic approach immediately suggests that $v_e \propto v^*\theta(\cos\theta_e - \cos\theta)$, which in the small angle approximation gives the Hoffman–de Gennes law $v_e \propto \theta(\theta^2 - \theta_e^2)$. The simplicity of this result conceals the fact that a no-slip boundary condition in the fluid mechanics of the problem leads to a force singularity [7–9].

A particularly simple experimental situation is the spreading of a small droplet of a non-volatile liquid on a surface it completely wets. Using the assumption of a small droplet spreading with a spherical cap shape and constant volume, the Hoffman–de Gennes law predicts a simple power law relationship for the dynamic contact angle $\theta \propto (t+t_o)^{-3/10}$ where t_o is a constant dependent on droplet volume and initial state; this power law is commonly referred to as Tanner's law, after the author who first derived it from the Navier–Stokes equations and experimentally confirmed it for the droplet spreading problem [10]. The corresponding power law for the radius, r_c, of the spherical cap is $r_c \propto (t+t_o)^{1/10}$. These power laws have been extensively investigated experimentally using small droplets of polydimethylsiloxane (PDMS) on silicon and glass substrates and found to be accurate descriptions of the data [1, 2]. In fact, the small angle approximation is usually very accurate up to contact angles of ~40° and can describe data with contact angles as high as 60° due to the cosine expansion using even powers [11]. This type of approach has also been used to describe the spreading of small stripes with circular arc cross-sections, where a power law $\theta \propto (t+t_o)^{-2/7}$, corresponding to $r_c \propto (t+t_o)^{1/7}$, was both predicted and observed [10, 12]; a result of practical importance in screen printing [13]. The hydrodynamic approaches also predict that the spreading of large droplets/puddles of liquids in the gravity regime will follow a power law of $r_c \propto (t+t_o)^{1/8}$ [14–16]. An alternative to the hydrodynamic view is to model droplet motion on the basis of the adsorption and desorption of molecules within the contact line region [17–19]. In this molecular-kinetic theory (MKT) the driving force remains a consequence of the out-of-balance interfacial tension forces $\gamma_{LV}(\cos\theta_e - \cos\theta)$, although the Hoffman–de Gennes law is no longer predicted in the small angle limit.

Spreading on smooth surfaces is a well-characterized situation and one that is accessible to study using simple droplet experiments. There is also a significant body of literature on the wetting of chemically patterned surfaces (for reviews see [20, 21]). One further question that naturally arises is how spreading might depend on surface topography. Surface topography is a factor in static wetting that has been extensively studied in recent years particularly because of the ability of high aspect ratio hydrophobic surface features to cause liquids to bridge between surface asperities and effectively cause a droplet to be suspended on the surface. These superhydrophobic surfaces originally came to prominence as self-cleaning and super-water repellent surfaces [22, 23], but can now be created using a wide range of materials approaches [24]. Often the behavior of droplets on these surfaces is well described by the Cassie–Baxter equation whose fundamental topographic control parameter is the solid surface fraction, φ_s [25–29]. Less well studied has been the effect of a rough hydrophilic surface to cause droplets to spread on surfaces on which they would normally form droplets. These super-wetting and hemi-wicking situations are a consequence of Wenzel's equation whose controlling topographic parameter is the surface roughness, r_s [30–32]. In these topographic cases with textured surfaces, the equilibrium contact angle, θ_T, is no longer that described by Young's law, but is one dependent on both the topography and the surface chemistry, e.g. $\theta_T(r_s, \varphi_s, \theta_e)$. Since at equilibrium the contact line ceases to move, the driving force for spreading can be expected to be $\gamma_{LV}(\cos\theta_T - \cos\theta)$ and so itself depend on topography [33]. Our previous work has suggested that such an effect can have dramatic consequences for both the Hoffman–de Gennes and Tanner laws [34, 35].

In this paper, we consider how surface texture might alter dynamic wetting. We begin by reviewing basic concepts from the statics of wetting and the Wenzel and Cassie–Baxter equations, including how this alters the conditions for a vanishing contact angle. We then consider how the topography modified driving force could alter the hydrodynamic model and molecular-kinetic theory of dynamic wetting. As part of these considerations, we take a simple dimensional analysis view to consider spreading of small droplets and stripes driven by capillary forces, and of large droplets with spreading driven by gravity. Finally, we review experiments for topography driven spreading of PDMS droplets on lithographically produced arrays of micro-posts [34, 35].

2. Topography and static wetting

2.1. Surface roughness and solid surface area fraction

Two of the key concepts relating to topography in static wetting are surface roughness and solid surface fraction. Surface roughness, r_s, is usually defined as the ratio of actual solid surface area to the planar projection of the solids surface area. The surface area fraction, φ_i, of a solid of surface chemistry type i with a Young's law contact angle θ_i is usually defined as the area of that type divided by the total surface area. However, these simple definitions can easily lead to ambiguities and do not emphasize the fact that they can change in value across a surface or that, in terms of droplets, it is their values at the contact line that determine local equilibrium [36]. By considering changes in surface free energy local to the contact

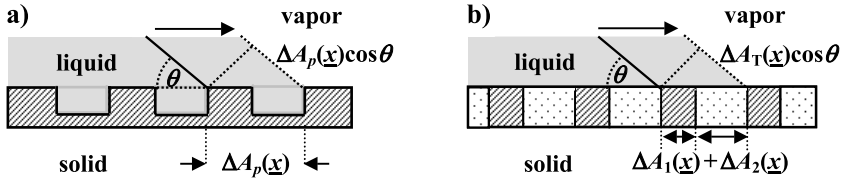

Figure 1. Changes in interfacial areas as the leading edge of a droplet advances by a small area, $\Delta A(\underline{x})$, across (a) a rough surface and (b) a composite surface of two types.

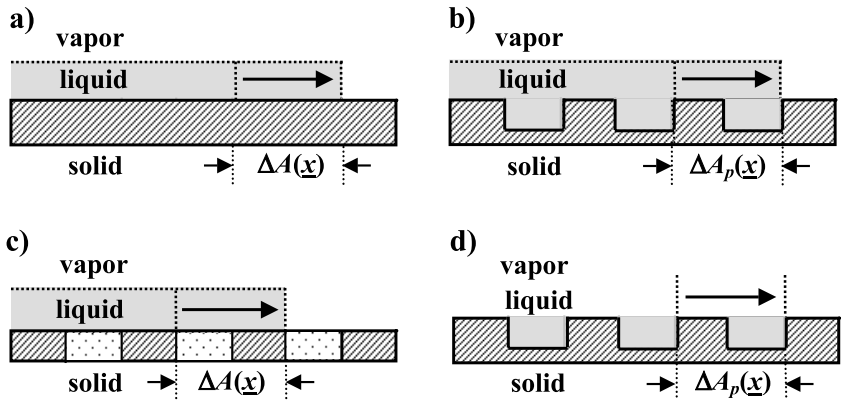

Figure 2. Changes in interfacial areas as a film of liquid advances by a small area across (a) a flat and smooth surface, (b) a rough surface and (c) a composite surface of two types of surface, and (d) shows the effect of a liquid advancing within the texture (hemi-wicking). In cases (c) and (d) the true area is related to the planar projection of area by $\Delta A(\underline{x}) = r_s(\underline{x})\Delta A_p(\underline{x})$, where $r_s(\underline{x})$ is the local roughness factor.

line it has been shown that the roughness and solid surface area fractions can be defined as local differential variables in the proximity of the three-phase contact line, $\underline{x}$,

$$r_s(\underline{x}) = \frac{\Delta A_{\text{wetted}}(\underline{x})}{\Delta A_p(\underline{x})} \tag{1}$$

where ΔA_{wetted} is a small change in wetted area that is sampled by a three-phase contact line and ΔA_p is the planar projection of that change. The corresponding definition of solid surface area fraction for a solid of surface type i is,

$$\varphi_i(\underline{x}) = \frac{\Delta A_i(\underline{x})}{\Delta A_T(\underline{x})} \tag{2}$$

where $\Delta A_i(\underline{x})$ is the change in wetted area of type i that can be sampled by a small three-phase contact line change $\Delta A_T(\underline{x}) = \Delta A_1(\underline{x}) + \Delta A_2(\underline{x})$ and the surface has been assumed to be composed of two types. Using these definitions and setting the surface free energy change due to a small advance at the contact line to zero gives rise to local forms of the Wenzel and Cassie–Baxter equations (figure 1) [36],

$$\cos\theta_W(\underline{x}) = r_s(\underline{x})\cos\theta_e(\underline{x}) \tag{3}$$

$$\cos\theta_{CB}(\underline{x}) = \varphi_1(\underline{x})\cos\theta_1(\underline{x}) + \varphi_2(\underline{x})\cos\theta_2(\underline{x}) \tag{4}$$

where $\theta_e(\underline{x})$, $\theta_1(\underline{x})$ and $\theta_2(\underline{x})$ each satisfy Young's law and the possibility that the surface chemistry (via the interfacial tensions) can vary across a surface has been indicated by the dependence on location, $\underline{x}$. More complex cases involving both changes in surface roughness and surface area fractions could be considered using the same approach, but these are not dealt with in this paper.

2.2. Surface roughness induced wetting

Not all liquids adopt an equilibrium droplet shape with a well-defined contact angle when deposited on a smooth and flat solid surface. Imagine a film of liquid advancing on a solid surface over a small additional area $\Delta A(\underline{x})$. The advancing liquid replaces a solid–vapor interface with a solid–liquid interface and so changes the surface free energy by $(\gamma_{SL} - \gamma_{SV})\Delta A(\underline{x})$ and at the same time the film of liquid has an increase in its liquid–vapor surface area so increasing the surface free energy by an additional $\gamma_{LV}\Delta A$ $(\underline{x})$ (figure 2(a)); the overall change in surface free energy is $\Delta F(\underline{x}) = (\gamma_{SL} - \gamma_{SV} + \gamma_{LV})\Delta A(\underline{x})$. If this advance reduces the surface energy the advance will continue until the surface is entirely wetted. Thus, the condition for complete wetting of a smooth and flat surface is that the spreading power, S, defined as $S = (\gamma_{SV} - \gamma_{SL} - \gamma_{LV})$ should be positive. When the spreading power is negative, so that a non-zero equilibrium contact angle exists, the spreading power can be written as $S = (\cos\theta_e - 1)\gamma_{LV}$ by using Young's law. On a rough surface, the argument can be repeated, but the roughness factor alters the contribution to the surface free energy change caused by replacing the solid–vapor interface by a solid–liquid interface (figure 2(b)). As a consequence, the condition for complete wetting becomes that $S_W(r) = r_s(\gamma_{SV} - \gamma_{SL}) - \gamma_{LV}$ should be positive. When the spreading power is negative, so that a non-zero equilibrium contact angle exists, the spreading power can be written as,

$$S_W(r_s) = (\cos\theta_W - 1)\gamma_{LV} \tag{5}$$

by using Wenzel's equation (equation (3)).

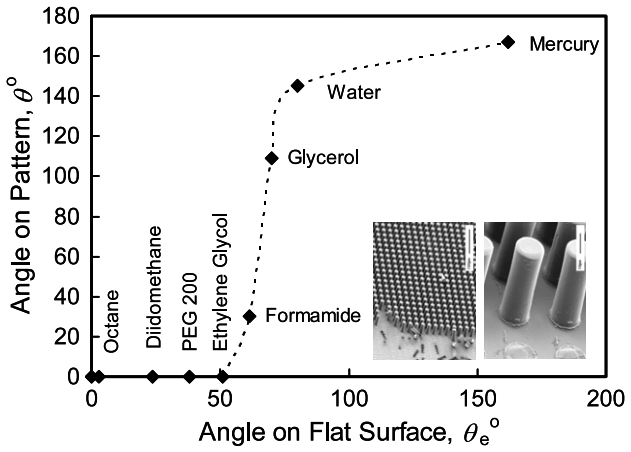

Figure 3. Contact angles for a range of liquids on a textured *SU*-8 surface. The inset shows scanning electron microscope images of the lithographically structured surfaces showing a square lattice of 15 μm diameter cylindrical pillars with a 30 μm lattice parameter (view of a field of pillars and a close-up view of the pillars). (Reprinted figure 2 from [32]. Copyright the Royal Society of Chemistry 2004.)

One immediate consequence of equations (3) and (5) is that liquids that would form partially wetting droplets with contact angles below 90° on a smooth solid surface of a given surface chemistry will spread further and display lower contact angles and in some cases, these droplets will not stop spreading and will eventually spread across the entire surface. Both of these conclusions have been confirmed experimentally [32]. Figure 3 shows the effect on the observed contact angle of changing the heights of polymer (*SU*-8 photoresist) micro-posts on a lithographically surface; the horizontal axis shows the observed contact angle on a smooth and flat surface of *SU*-8. These surfaces were composed of square lattices of 15 μm diameter cylindrical pillars with a 30 μm lattice parameter in a polymer photoresist (inset figure 3). For droplets of water, the effect of the surface structure is to increase the contact angle due to the inability of the water to penetrate between the posts, thus giving a Cassie–Baxter superhydrophobic effect. However, for formamide the effect of surface structure is to reduce the observed contact angle and for liquids with even lower contact angles on the flat *SU*-8, the effect is to completely spread out and imbibe the liquid. For these liquids, topography reinforces the tendency towards wetting arising from the surface chemistry and it can be said to be driving the spreading.

On a composite Cassie–Baxter surface consisting of two surface types, the surface free energy change caused by replacing the solid–vapor interface across one period of the surface by a solid–liquid interface also changes the spreading power (figure 2(c)). When the spreading power is negative, so that a non-zero equilibrium contact angle exists, the spreading power can be written as,

$$S_{\mathrm{CB}}(\varphi_1, \varphi_2) = (\cos\theta_{\mathrm{CB}} - 1)\gamma_{\mathrm{LV}}. \tag{6}$$

Another situation, called hemi-wicking, can occur in which the topography drives a complete imbibition of a droplet by the surface. In this case the liquid spreads within the texture of the surface, but does not cover the tops of the asperities (figure 2(d)). In the simple case of flat topped surface features, Quéré *et al* have shown that the condition for the liquid to spontaneously advance within the surface texture is [37, 38],

$$\left(\frac{r_{\mathrm{s}} - \varphi_{\mathrm{s}}}{1 - \varphi_{\mathrm{s}}}\right)(\gamma_{\mathrm{SV}} - \gamma_{\mathrm{SL}}) - \gamma_{\mathrm{LV}} > 0 \tag{7}$$

which can be written as a hemi-wicking spreading power,

$$S_{\mathrm{HW}}(r_{\mathrm{s}}, \varphi_{\mathrm{s}}) = \left(\left(\frac{r_{\mathrm{s}} - \varphi_{\mathrm{s}}}{1 - \varphi_{\mathrm{s}}}\right)\cos\theta_{\mathrm{e}} - 1\right)\gamma_{\mathrm{LV}}. \tag{8}$$

This condition also implies that hemi-wicking will not occur provided,

$$\varphi_{\mathrm{s}} > \frac{1 - \cos\theta_{\mathrm{W}}}{1 - \cos\theta_{\mathrm{e}}}. \tag{9}$$

2.3. Solid–liquid composite surface induced wetting

The Cassie–Baxter equation is commonly used to explain the enhancement of partial wetting into superhydrophobicity. A simple view is to imagine a post type surface structure with a droplet only able to advance across the tops of the posts and bridge across the gaps between them. Effectively in equation (4), $\theta_1(\underline{x})$ is the Young's law contact angle, θ_{e}, for the solid and $\theta_2 = 180°$ is the contact angle of the liquid in contact with air. At the same time the surface area fraction for the solid is φ_{s} and for the gaps between the posts the area fraction is $(1 - \varphi_{\mathrm{s}})$, thus giving,

$$\cos\theta_{\mathrm{CB}} = \varphi_{\mathrm{s}}\cos\theta_{\mathrm{e}} - (1 - \varphi_{\mathrm{s}}). \tag{10}$$

However, we can also imagine an alternative situation in which a surface has been subject to hemi-wicking and a droplet then advances across the tops of the solid posts and the liquid already contained between these posts. In this case, $\theta_2 = 0°$ is the contact angle of the liquid in contact with itself, so that the Cassie–Baxter equation gives,

$$\cos\theta^1_{\mathrm{CB}} = \varphi_{\mathrm{s}}\cos\theta_{\mathrm{e}} + (1 - \varphi_{\mathrm{s}}). \tag{11}$$

The resulting contact angle for the droplet is lower than it would be simply on the solid surface. Equation (11) also allows the condition for a liquid not to hemi-wick (equation (9)) to be stated in terms of Wenzel's equation as,

$$\cos\theta_{\mathrm{W}} < \cos\theta^1_{\mathrm{CB}}. \tag{12}$$

For Young's law contact angles less than 90° this implies that the Wenzel contact angle needs to be larger than the contact angle predicted for a droplet on the composite surface of the solid with liquid between the surface features.

2.4. Maximal droplet thickness

One aspect of static wetting that does not appear to have been commented upon in the recent literature is the effect of topography on large droplets ($r_{\mathrm{c}} \gg \kappa^{-1}$). In this case, the droplet becomes flattened due to gravity and the shape is a

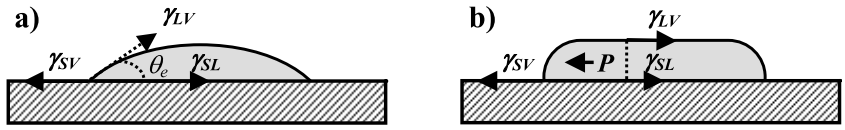

Figure 4. Equilibrium shapes of (a) small droplets ($r_c \ll \kappa^{-1}$) and (b) large puddles ($r_c \gg \kappa^{-1}$). After [15].

thick puddle of thickness h_c (figure 4) [14–16]. The balance of horizontal forces on a rough surface then gives,

$$r_s\gamma_{SV} = \gamma_{LV} + r_s\gamma_{SL} - \frac{\rho g h_c^2}{2} \tag{13}$$

where the last term is from the hydrostatic pressure integrated over the thickness h_o. Using Wenzel's equation we find,

$$h_c = 2\kappa^{-1}\sin(\theta_W/2) \approx \kappa^{-1}\theta_W \tag{14}$$

where the final approximation is in the limit of small Wenzel angles. Thus, Wenzel's equation for Young's law contact angles less than 90° implies that in the limit of large droplet volumes the maximal droplet height is reduced. For a Cassie–Baxter composite surface composed of the liquid and the solid, our expectation is that

$$h_c = 2\kappa^{-1}\sin(\theta^l_{CB}/2) \approx \kappa^{-1}\theta^l_{CB}. \tag{15}$$

Since volume must be conserved, a rough (or a composite solid–liquid) surface should cause a droplet possessing $\theta_e < 90°$ to adopt a thinner pancake shape with a larger lateral extent than it would on a flat and smooth solid surface of the same material. Effectively, Wenzel roughness results in stronger spreading tendencies and the condition $r_c \sim \kappa^{-1}$ is no longer sufficient to define the cross-over from the gravity regime to the capillary regime, which now is expected to occur at larger sizes. It is unclear what the cross-over condition should be, but one possibility suggested by equation (13) is $r_c \sim r_s\kappa^{-1}$.

The surface free energy approach outlined in this section assumes that the wetting of the surface does not follow the symmetries of its small scale structure, but is an average effect around the contact perimeter which remains circular. However, droplets on textured surfaces do under some circumstances adopt the symmetries of the underlying lattice with coordinated movements of contact lines leading to faceted droplets; the assumption of a circular contact perimeter is therefore quite coarse [39]. Our approach also ignores the difference between the theoretical Young's law contact angle and the experimentally observed advancing and receding contact angles. However, in our opinion it is nonetheless a useful view in providing some underlying guiding principles.

3. Topography and spreading

3.1. Rate of change of surface free energy

Our previous considerations on the influence of topography on wetting statics shows that under some circumstances the final contact angle can be lower than predicted by Young's law (topography driven spreading) and that droplets that only partially spread on a smooth and flat surface may spread completely and not reach an equilibrium droplet shape at all (topography driven wetting). The same considerations also suggest that the rate of change of surface free energy occurring at the contact line, and hence wetting dynamics, will be modified by topography. For example, if a contact line advances over a rough surface, but at all locations retains contact with the solid (the Wenzel situation), the surface free energy change is, $\Delta F(\underline{x}) = [r_s(\underline{x})(\gamma_{SL} - \gamma_{SV}) + \gamma_{LV}\cos\theta]\Delta A_p(\underline{x})$. Assuming the droplet remains axially symmetric so that $\Delta A(\underline{x}) = 2\pi\Delta r_c$, where r_c is the planar contact radius, and defining a radial edge speed as $v_e = \mathrm{d}r_c/\mathrm{d}t$, the rate of change of surface free energy with respect to time is given as,

$$\dot{F}(\underline{x}) = 2\pi r_c\gamma_{LV}(\cos\theta - \cos\theta_W)\, v_e \tag{16}$$

where the combination of interfacial tensions has been replaced using Wenzel's equation. This assumes that hemi-wicking has not occurred in advance of the droplet edge (i.e. the droplet spreads on a dry surface). Similarly, on a surface with two types of surface chemistry represented by Young's law contact angles of θ_1 and θ_2, and with surface fractions φ_1 and φ_2, the rate of change of surface free energy is,

$$\dot{F}(\underline{x}) = 2\pi r_c\gamma_{LV}(\cos\theta - \varphi_1\cos\theta_1 - \varphi_2\cos\theta_2)\, v_e. \tag{17}$$

In the special case that the composite surface involves a solid of surface fraction φ_s and Young's law contact angle of θ_s with the dry solid separated by gaps already filled by the liquid, so that the liquid surface fraction is $(1 - \varphi_s)$, equation (17) becomes,

$$\dot{F}(\underline{x}) = 2\pi r_c\gamma_{LV}\left(\cos\theta - \cos\theta^l_{CB}\right) v_e \tag{18}$$

where $\cos\theta^l_{CB}$ is defined by equation (11).

An alternative view of equations (16)–(18) is to regard the contact line on a textured surface as subject to an effective out-of-balance force per unit length of contact line of $\gamma_{LV}(\cos\theta - \cos\theta_T)$, where θ_T is either the Wenzel contact angle, θ_W, or the Cassie–Baxter contact angle, θ^l_{CB}, for a composite solid–liquid surface and is determined by the surface topography. Thus, we might expect that not only would the final equilibrium contact angle be lower, but the rate at which a droplet evolves to that state would be faster due to a larger effective spreading force induced by the topography. However, what is not taken into account in these considerations is how the opposition to spreading is modified by the topography. Spreading involves a flow and any strong roughness or surface texture could significantly alter the flow pattern, thus modifying the viscous dissipation. Alternatively, if we consider the motion of the

contact line to arise from the balance between adsorption and desorption of molecules, changes in solid surface area could modify the balance between these processes. The net effect of surface topography on wetting dynamics is, therefore, far from obvious, but this type of approach does enable some of the possible factors to be identified and discussed.

3.2. Hydrodynamics

In cylindrical coordinates $(r,\ \phi,\ z)$ and assuming axial symmetry, the rate of dissipation of energy in a spreading fluid is given by,

$$T\dot{S} = \eta \int_{\text{liquid}} \left\{ 2\left[\left(\frac{\partial v_r}{\partial r}\right)^2 + \left(\frac{v_r}{r}\right)^2 + \left(\frac{\partial v_z}{\partial z}\right)^2 \right] + \left[\frac{\partial v_r}{\partial z} + \frac{\partial v_z}{\partial r} \right]^2 \right\} \mathrm{d}\Omega \tag{19}$$

where the integral is over the fluid volume and v_r and v_z are the radial and axial velocity components and the velocity field also satisfies the continuity equation [40]. Given a velocity field for the fluid it is then possible to evaluate the rate of energy dissipation in the flow of the fluid and equate it to the rate of change of surface free energy.

3.2.1. Dimensional analysis. McHale *et al* have argued that a simple estimate of the rate of energy dissipation on a flat and smooth surface can be obtained by considering the characteristic dimensions in equation (19) [11]. This suggests that for a small spherical cap shaped droplet the dominant terms in the integrand of equation (19) are those of the form $v_e^2 r_c^2 / h_c$, corresponding to the term involving $(\partial v_r/\partial z)^2$, where r_c is the radius of the droplet and h_c is maximal height of the droplet. For a spherical cap shape $h_c/r_c = \tan(\theta/2)$ and so the expected form of the dissipation was suggested to be of the form,

$$T\dot{S} = \frac{2\pi\, r_c \eta v_e^2}{k \tan(\theta/2)} \tag{20}$$

where k is a constant dependent on the choice of the fluid velocity field and the geometry over which dissipation occurs. It seems plausible that the constant k would also depend on the surface roughness and/or the solid surface fraction and so we can write $k = k(r_s, \varphi_s)$; whether or not this might also introduce a weak dependence on the Young's law equilibrium or the dynamic contact angles is not clear in this approach. To obtain the edge speed we now equate equation (16) or (18) with equation (20),

$$v_e = k(r_s, \varphi_s) v^* (\cos\theta_T(r_s, \varphi_s) - \cos\theta) \tan(\theta/2) \tag{21}$$

where $\theta_T(r_s, \varphi_s)$ is either the Wenzel contact angle, θ_W, or the Cassie–Baxter contact angle, θ^1_{CB}, for a composite solid–liquid surface. For the Wenzel case, using a small angle expansion then gives,

$$v_e \approx \tfrac{1}{2} k(r_s) v^* ((r_s - 1) + \tfrac{1}{2}(\theta^2 - r_s \theta_e^2))\theta + \cdots \tag{22}$$

whereas the composite solid–liquid case gives,

$$v_e \approx \tfrac{1}{4} k(\varphi_s) v^* (\theta^2 - \varphi_s \theta_e^2)\theta + \cdots. \tag{23}$$

When the roughness vanishes ($r_s \to 1$) or the solid surface fraction tends to 100% ($\varphi_s \to 1$), equations (22) and (23) tend to the Hoffman–de Gennes cubic-type form for the relationship between edge speed and dynamic contact angle. However, if there is roughness ($r_s > 1$) then equation (22) implies that a linear term in dynamic contact angle will become apparent. In the case of composite solid–liquid surface with most of the surface filled by the liquid ($\varphi_s \to 0$), equation (23) implies that dependence on the equilibrium contact angle vanishes and a cubic relationship, similar to spreading on a complete wetting surface, will become apparent.

There are some strong assumptions in this type of approach to describing dynamic wetting. For example, it has been assumed that hemi-wicking either does not occur or that the contribution it makes to the dissipation is small. If this were not the case, terms of the form $(\partial v_r/\partial r)^2$ could become important. Physically this might be indicated by a droplet centered on a far wider film of liquid within the texture of the substrate. The dynamics for imbibition into a textured surface composed of a forest of micropillars by a film (i.e. pure hemi-wicking) have been described by Ishino *et al* [41]. Another case might be where the droplet no longer maintains an axially symmetric shape, but becomes influenced by the underlying symmetry of the texture of the surface.

3.2.2. Dissipation in a wedge. Motivated by an analysis of flow patterns in a simple wedge advancing at a constant velocity and contact angle [42], de Gennes *et al* derived a formula for viscous dissipation [1, 6, 43]. In the simplest approach, he assumed that Poiseuille flow occurs within a macroscopic wedge shaped region extending from x_o to x_1 (figure 5(a)). The liquid velocity field is then,

$$v_x(x, z) = v_e \left(\frac{z}{h(x)}\right)\left(2 - \left(\frac{z}{h(x)}\right)\right). \tag{24}$$

This form of velocity field ensures a no-slip boundary condition at the solid surface and vanishing shear stress at the free liquid surface; it also gives an averaged velocity over the depth, $h(x)$, of the fluid of $v_A = 2v_e/3$. The viscous dissipation in the two-dimensional wedge scaled by the perimeter length, $2\pi r_c$, is then given by,

$$T\dot{S}_{\text{wedge}} = 2\pi\eta r_c \int_{x_o}^{x_1} \int_0^{h(x)} \left(\frac{\mathrm{d}v_x}{\mathrm{d}z}\right)^2 \mathrm{d}z\, \mathrm{d}x = \frac{8\pi\eta r_c v_e^2 L}{3\tan\theta} \tag{25}$$

where $L = \log_e |l/\varepsilon|$ with $l = x_1 - x_0$ and ε is the truncation length defined in figure 5(a), removes a mathematical singularity close to the contact line [1, 7–9, 42]. A similar result including a logarithmic cut-off can be derived using a spherical cap shaped droplet with dissipation in a cone shaped region inscribed within the droplet although the $\tan\theta$ factor is replaced by $\tan\theta/2$ [11]. For simple liquids without slippage ε is a molecular cut-off length. A calculation including a slip boundary condition allowing the liquid to move with a finite velocity at the solid surface has been carried out due to its applicability to polymer melts and the cut-off is then $\varepsilon = b/\theta$, where b is the slip length and can depend on velocity [1, 44]. The slip length is the distance to the surface at

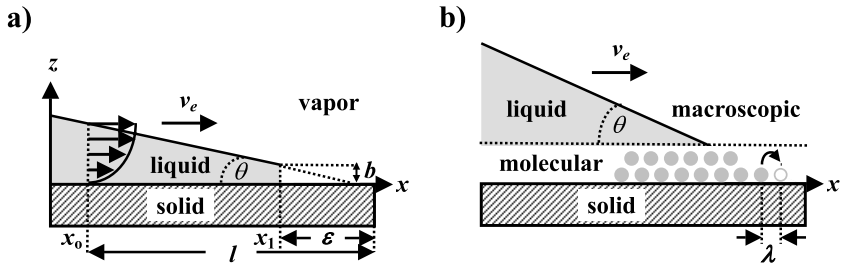

Figure 5. (a) Hydrodynamic model with Poiseuille flow occurring within a macroscopic wedge shaped region close to the contact line, and (b) molecular-kinetic theory with adsorption and desorption processes.

which the velocity extrapolates to zero and is formally defined as $b = v_x/(\mathrm{d}v_x/\mathrm{d}z)_{z=0}$. It is possible that surface texture would be an alternative mechanism defining the cut-off so that the logarithmic factor would depend on the roughness and/or solid surface fraction, i.e. $L = L(r_s, \varphi_s)$. Using equation (16) or (18) and this viscous dissipation in a wedge approach, the edge speed is given by,

$$v_e = \frac{3v^*}{4L(r_s, \varphi_s)}(\cos\theta_T(r_s, \varphi_s) - \cos\theta)\tan\theta \qquad (26)$$

which is similar to equation (21) apart from the presence of the half-angle in the tan( ) factor. To match equation (26) to equation (21) in the small angle approximation, an effective $k(r_s, \varphi_s) = 3/(2L(r_s, \varphi_s))$ can be defined. Using the alternative approach of a cone inscribed within a spherical cap to estimate viscous dissipation results in a $\tan(\theta/2)$ dependence and this gives an edge speed–dynamic contact angle relationship with good accuracy for larger contact angles [11]. The implication of equation (26) is that because for any given texture the cut-off function is a constant in dynamic contact angle, equations (22) and (23) predict the dependence of edge speed on dynamic contact angle (in the small angle approximation). Because the contact angle dependence is through a product of $\cos\theta$ that expands in even powers and $\tan\theta$ that expands in odd powers, the first order term in a small angle expansion is accurate to within 10% even at contact angles as high as 45°.

3.2.3. Gravity regime. To estimate what might happen in the limit of a large puddle ($r_c \gg \kappa^{-1}$), we first follow Brochard-Wyart *et al*'s argument for dissipation controlled by the bulk [15]. The gain of gravitational energy is,

$$\frac{\mathrm{d}E_g}{\mathrm{d}t} = -\rho g(\dot{h}_c/2)\Omega \qquad (27)$$

where Ω is the volume of liquid. Using a radial velocity field $v(r) = (r/r_c)v_e$, they argued that the bulk dissipation is,

$$T\dot{S}_{\mathrm{Bulk}} = \frac{3\pi r_c^2 \eta v_e^2}{2h_c} \qquad (28)$$

and then imposing mass conservation using the approximation for the volume of $\Omega \cong \alpha\pi r_c^2 h_c$, where α is a constant of order unity, found,

$$v_e \cong v^*\left(\frac{2\kappa^2\Omega^3}{3\alpha^2\pi^3}\right)\frac{1}{r_c^7}. \qquad (29)$$

Since surface roughness and solid surface fraction would not alter equation (27) and for large drops the radial velocity field would not change, equation (29) would appear to remain valid. Since it does not involve changes due to surface topography, it is not obvious from this approximate approach how surface topography changes the rate of spreading of a large droplet if its spreading is controlled by the bulk dissipation.

3.2.4. Molecular-kinetic theory. An alternative to the hydrodynamic model is one based on the adsorption and desorption of molecules in a microscopic region close to the contact line [17–19]. In this molecular-kinetic model due to Blake and Haynes [17], it was suggested that the contact line motion is due to a stress-modified activated rate process. In equilibrium with no contact line motion, molecules are in constant motion jumping from one adsorption site on the substrate to another over average distances of λ at a typical frequency of $K_o \propto \exp(-W/k_BT)$, where W is an activation energy and k_BT is the Boltzmann thermal energy (figure 5(b)); in general it is assumed that $\lambda \sim 1/n^{1/2}$ where n is the number of adsorption sites per unit area. Out of equilibrium, molecules jump forward and backward with different frequencies K_+ and K_- resulting in a contact line velocity of $v_e = \lambda(K_+ - K_-)$. Due to the shear stress, the energy barriers to molecular motion are lowered by $w/2n$ in the forward direction and raised by $w/2n$ in the reverse direction, where w is the work done by the shear stress per unit displacement of unit length of the contact line. The contact line velocity due to the difference in jump frequencies is then,

$$v_e = \lambda\,(K_+ - K_-) = 2\lambda K_o \sinh\left(\frac{w}{2nk_BT}\right). \qquad (30)$$

On a smooth and flat surface, the model assumes that the shear stress driving the contact line motion is the out-of-balance interfacial tension force $\gamma_{LV}\,(\cos\theta_e - \cos\theta)$, thus giving,

$$v_e = 2\lambda K_o \sinh\left(\frac{\gamma_{LV}\,(\cos\theta_e - \cos\theta)}{2nk_BT}\right). \qquad (31)$$

Equation (31) suggests $v_e \propto (\theta^2 - \theta_e^2)$ in the small angle limit and so does not reduce to the cubic-type Hoffman–de Gennes form, although it has often been found to fit experimental data for simple liquids reasonably well providing the molecular parameters are chosen suitably [19, 45]. As

noted by de Ruijter *et al* [46], when the argument of the exponential is small, v_e is directly proportional to the driving force $\gamma_{LV}(\cos\theta_e - \cos\theta) \approx \gamma_{LV}(\theta^2 - \theta_e^2)/2$ with a constant of proportionality of $\zeta_o^{-1} = nk_BT/K_o\lambda = k_BT/K_o\lambda^3$ which can be interpreted as a friction coefficient per unit length of the contact line.

The molecular-kinetic model offers an alternative to the hydrodynamic model and includes molecular parameters whose values are expected to be of the order of $\lambda \sim 1$ nm and $K_o \sim 10^6\ s^{-1}$ for viscous flow of simple liquids. However, it is far from clear how surface topography or surface heterogeneity would modify the molecular-kinetic model and few authors appear to have considered this problem. Petrov *et al* considered how the model might be modified to account for wetting dynamics on a smooth heterogeneous surface composed of two types of surface chemistry and obtained a formula involving two terms of the form of equation (31) [47]. However, such a formula does not transparently account for the net shear stress arising from the out-of-balance interfacial tension force involving the Wenzel or Cassie–Baxter contact angle. In our opinion, an intuitive approach would be to assume that both the equilibrium jump frequency K_o and the number of adsorption sites per unit area n (and hence the average distance of $\lambda \sim 1/n^{1/2}$ between jumps) depend on the surface texture, i.e. $K_o = K_o(r_s, \varphi_s)$, $n = n(r_s, \varphi_s)$ and $\lambda = \lambda(r_s, \varphi_s)$. It seems possible that these parameters could depend on the Young's law contact angle, but less likely that there would be a strong dependence on the dynamic contact angle. The shear stress activation of the contact line motion would involve the observed equilibrium contact angle (i.e. either the Wenzel or Cassie–Baxter contact angle) and this would result in a modification of the edge speed to,

$$v_e = 2\lambda(r_s, \varphi_s)K_o(r_s, \varphi_s)\sinh\left(\frac{\gamma_{LV}(\cos\theta_T(r_s, \varphi_s) - \cos\theta)}{2n(r_s, \varphi_s)k_BT}\right). \tag{32}$$

A consequence of equation (32) is that if a Wenzel roughness effect is assumed and the argument of the exponential and the cosine's expanded, the edge speed then becomes,

$$v_e \approx \left(\frac{\gamma_{LV}}{\zeta_o}\right)[(r_s - 1) + (\theta^2 - r_s\theta_e^2)/2] \tag{33}$$

which has a constant first term. Effectively, the friction coefficient becomes part of a driving force term and so causes a topography driven wetting. It is also possible to use a molecular-kinetic theory approach to address the question of a slip boundary condition, although this is not addressed in this current report [48].

One of the conclusions from the original molecular-kinetic theory (equation (31)) was the prediction for forced wetting of maximum and minimum velocities corresponding to dynamic contact angles of 180° and zero, respectively. Above the maximum velocity, air entrainment is predicted and this effect is observed experimentally at high coating speeds [18]. Equation (32) also predicts a maximum velocity for wetting the surface given by,

$$v_{180} = 2\lambda(r_s, \varphi_s)K_o(r_s, \varphi_s)\sinh\left(\frac{\gamma_{LV}(\cos\theta_T(r_s, \varphi_s) + 1)}{2n(r_s, \varphi_s)k_BT}\right) \tag{34}$$

and a maximum for dewetting the surface of,

$$-v_o = 2\lambda(r_s, \varphi_s)K_o(r_s, \varphi_s)\sinh\left(\frac{\gamma_{LV}(1 - \cos\theta_T(r_s, \varphi_s))}{2n(r_s, \varphi_s)k_BT}\right). \tag{35}$$

Assuming a Wenzel roughness with a Young's law contact angle less than 90°, equation (34) implies higher coating speeds would be possible providing the liquid retained contact with the surface features and did not convert to a Cassie–Baxter solid–air type situation as coating speed increased.

4. Power laws in dynamic wetting

4.1. Spherical cap droplet

A classic experiment demonstrating the cubic dependence on contact angle of the edge speed is the spreading of a small droplet of polydimethylsiloxane (PDMS) oil on a glass or a silicon substrate [2, 10]. PDMS has a wide range of viscosities with relatively constant density ($\rho \sim 9.71\ kg\ m^{-3}$) and surface tension ($\gamma_{LV} \sim 20\ mN\ m^{-1}$) so allowing the capillary length to be kept constant (~1.4 mm) whilst varying the characteristic speed over many orders of magnitude. Moreover, because PDMS is non-volatile, its volume, Ω, is conserved and because the equilibrium contact angle, θ_e, vanishes, it is possible to solve $v_e = v_e(\theta)$ and obtain power law dependencies in time for various geometric parameters. For a spherical cap shape, the defining equations for the geometry are,

$$r_c = R\sin\theta, \qquad h_c = R(1 - \cos\theta), \qquad R = \left(\frac{3\Omega}{\pi\beta(\theta)}\right)^{1/3} \tag{36}$$

where,

$$\beta(\theta) = (1 - \cos\theta)^2(2 + \cos\theta). \tag{37}$$

Using small angle expansions for the spherical cap allows the geometric parameters to be written as,

$$r_c \approx \left(\frac{4\Omega}{\pi\theta}\right)^{1/3}, \qquad h_c \approx \left(\frac{\Omega\theta^2}{2\pi}\right)^{1/3}, \qquad R \approx \left(\frac{4\Omega}{\pi\theta^4}\right)^{1/3} \tag{38}$$

and so the edge speed, $v_e = dr_c/dt$ is given by,

$$v_e = \frac{dr_c}{dt} \approx -\frac{1}{3}\left(\frac{4\Omega}{\pi\theta^4}\right)^{1/3}\left(\frac{d\theta}{dt}\right). \tag{39}$$

Considering the small angle expansions given by equations (22) and (23) and defining $\alpha(r_s)$ to have the value of $\frac{1}{4}$ or $(r_s - 1)/2$ accordingly, we can write the topography modified edge speed as,

$$v_e \approx \alpha(r_s)k(r_s, \varphi_s)v^*\theta^p \tag{40}$$

where the exponent, p, depends on the surface topography. Combining with equation (39) and solving gives the power law

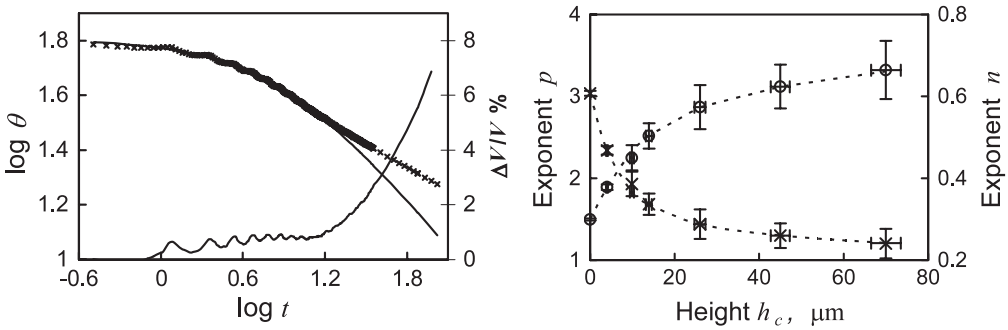

Figure 6. (a) A log–log plot of the dynamic contact angle and time with a fit of $\theta \propto 1/(t+t_o)^{0.614}$ for the spreading of a 10 000 cSt viscosity polydimethylosiloxane droplet on an *SU*-8 textured surface with 15 μm diameter pillars of height 45 μm and lattice parameter 30 μm; the percentage change in drop volume is also shown (lower curve and right-hand axis). (b) Exponents p and n extracted from the edge speed–dynamic contact angle data ($\times\times\times$, left axis) and dynamic contact angle-time (ooo, right axis) with increasing pillar height. (Reprinted figures 3 and 4 from [34]. Copyright the American Physical Society 2004.)

dependence,

$$\theta(t) \approx \left[\left(\frac{1}{3p+1}\right)\left(\frac{1}{\alpha(r_s)k(r_s,\varphi_s)v^*}\right)\left(\frac{4\Omega}{\pi}\right)^{1/3}\right]^{3/(3p+1)} \times \left(\frac{1}{t+t_o}\right)^{3/(3p+1)} \tag{41}$$

where t_o is a constant of integration. In the small angle approximation, equation (38) implies $r_c \propto \Omega^{1/3}\theta^{-1/3}$, $h_c \propto \Omega^{1/3}\theta^{2/3}$ and $R \propto \Omega^{1/3}\theta^{-4/3}$, so that if $v_e \propto \theta^p$, the power laws of the geometric parameters with time are,

$$\begin{aligned} \theta &\propto (t+t_o)^{-3/(3p+1)} & r_c &\propto (t+t_o)^{1/(3p+1)} \\ h_c &\propto (t+t_o)^{-2/(3p+1)} & R &\propto (t+t_o)^{4/(3p+1)}. \end{aligned} \tag{42}$$

When the surface is both flat and smooth or a Cassie–Baxter composite solid–liquid surface so that $p = 3$, the exponents are $-3/10$, $1/10$, $-1/5$ and $4/10$, respectively. If the surface is rough, and the edge velocity tends to linear in contact angle (i.e. towards $p = 1$), the expectation is that these exponents will tend towards $-3/4$, $1/4$, $-1/2$ and 1, respectively [33]. As discussed in section 2 on static wetting, there are some strong assumptions including maintenance of an axially symmetric droplet shape, absence of hemi-wicking and a lack of dynamic contact angle dependence entering into the cut-off for the viscous dissipation, $L(r_s, \varphi_s)$.

One systematic experimental study on the influence on the spreading of droplets due to a variation in height of micro-posts arranged in a lattice on a surface has been reported in the literature [34, 35]. In that study the surface was composed of circular *SU*-8 polymer micro-posts of diameter 15 μm arranged in a square array with post-to-post separation of 30 μm. Each surface had a uniform height set of micro-posts with the maximum height used being 70 μm. On the surface with the tallest micro-posts, droplets of water balled up and were observed to be in the suspended Cassie–Baxter solid–air state, thus demonstrating that the surface topography had a major effect on static wetting by water. The spreading experiments were conducted used video profilometry of droplets of 10 000 cSt PDMS oil of initial volume $\sim$1 μl. Droplets were observed to spread with well-defined dynamic contact angles from over 70° down to around 30° before entering a phase of spreading in which the dominant process was imbibition within the surface texture. Figure 6(a) shows an example of the change in contact angle with time over this initial spreading period. The lower curve in figure 6(a) shows the change in volume as estimated from the droplet profile. The constant volume in the initial period supports the view that in the initial stages droplet spreading dominates; the upper solid curve shows a fit to $\theta = B(t+t_o)^{-n}$ over this initial constant volume period. The edge speed was also estimated from the droplet profiles and fitted to $v_e = D(t+t_o)^p$. Figure 6(b) shows the change in the exponents n and p as the height of the micro-posts was increased. The exponent n changes from 3/10 towards 3/4 and the exponent p changes from 3 towards 1, consistent with equation (42) based on spreading drive by a Wenzel roughness.

4.2. Large droplets/puddles

When the droplet size becomes much greater than the capillary length, the droplet becomes flattened into a puddle and when the spreading is controlled by dissipation in the bulk the edge speed is proportional to r_c^{-7}, which appears to be independent of surface topography. The puddle radius, r_c, should then follow a $(t+t_o)^{1/8}$ power law in time with a puddle thickness following $h_c \propto (t+t_o)^{-1/4}$. Neither the prediction in section 2.4 of surface roughness influence on the maximal droplet thickness, nor the prediction that the edge speed will be independent of thickness for large puddles, appear to have been tested experimentally.

4.3. Small stripes of liquids

An alternative to experiments using axially symmetric droplets is to perform liquid spreading using a stripe shape with a circular arc cross-section [12]. For a stripe with cross-section much less than the capillary length, the geometry can be defined using a circular radius R, a maximal height h_c, and a contact width $2r_c$. The defining equations for this geometry

are then,

$$r_c = R\sin\theta, \qquad h_c = R(1-\cos\theta),$$
$$R = \left(\frac{A}{\theta - \sin\theta\cos\theta}\right)^{1/2} \tag{43}$$

where A is the area of the circular cap, which for the spreading of a non-volatile liquid is a constant. Using small angle expansions allows the geometric parameters to be written as,

$$r_c \approx \left(\frac{3A}{2\theta}\right)^{1/2}, \qquad h_c \approx \left(\frac{3A\theta}{8}\right)^{1/2}, \qquad R \approx \left(\frac{3A}{2\theta^3}\right)^{1/2} \tag{44}$$

so that the edge speed, $v_e = \mathrm{d}r_c/\mathrm{d}t$ is given by,

$$v_e = \frac{\mathrm{d}r_c}{\mathrm{d}t} \approx -\frac{1}{2}\left(\frac{3A}{2\theta^3}\right)^{1/2}\left(\frac{\mathrm{d}\theta}{\mathrm{d}t}\right). \tag{45}$$

Using the topography modified edge speed relation given by equation (40), i.e. $v_e \propto \theta^p$, and solving gives the power law dependence,

$$\theta(t) \approx \left[\left(\frac{2p+1}{\alpha(r_s)k(r_s,\varphi_s)v^*}\right)\left(\frac{3A}{2}\right)^{1/2}\right]^{2/(2p+1)} \times \left(\frac{1}{t+t_o}\right)^{2/(2p+1)}. \tag{46}$$

In the small angle approximation, equation (44) implies $r_c \propto A^{1/2}\theta^{-1/2}$, $h_c \propto A^{1/2}\theta^{1/2}$ and $R \propto A^{1/2}\theta^{-3/2}$, and so that if $v_e \propto \theta^p$, the power laws of the geometric parameters with time are,

$$\theta \propto (t+t_o)^{-2/(2p+1)} \qquad r_c \propto (t+t_o)^{1/(2p+1)}$$
$$h_c \propto (t+t_o)^{-1/(2p+1)} \qquad R \propto (t+t_o)^{3/(2p+1)}. \tag{47}$$

When the surface is both flat and smooth or a Cassie–Baxter composite solid–liquid surface so that $p = 3$, the exponents are $-2/7$, $1/7$, $-1/7$ and $3/7$, respectively. If the surface is rough, and the edge velocity tends to linear in contact angle (i.e. towards $p = 1$), the expectation is that these exponents will tend towards $-2/3$, $1/3$, $-1/3$ and 1, respectively. These predictions, which may have implications for printing on rough surfaces [13], have not been experimentally tested.

4.4. Approach to equilibrium of a droplet

In section 4.1 the effect of surface texture on power law spreading for small droplets completely wetting the surface was considered. In the case that a droplet spreads maintaining its volume constant, but the eventual equilibrium remains a droplet, we can show that an exponential approach to equilibrium would be expected. The edge speed obtained from equation (36) can be written as,

$$v_e = -G(\theta)\left(\frac{\mathrm{d}\theta}{\mathrm{d}t}\right) \tag{48}$$

where the function $G(\theta)$ is defined by the spherical cap shape as,

$$G(\theta) = -\left(\frac{3\Omega}{\pi}\right)^{1/3}\frac{\mathrm{d}}{\mathrm{d}\theta}\left[\frac{\sin\theta}{\beta(\theta)}\right] = \left(\frac{3\Omega}{\pi}\right)^{1/3}\frac{1}{(2+\cos\theta)^{4/3}(1-\cos\theta)^{2/3}}. \tag{49}$$

We now choose the hydrodynamic model for viscous dissipation and use equation (26) with equation (48) to obtain,

$$\left(\frac{\mathrm{d}\theta}{\mathrm{d}t}\right) = -\left(\frac{3v^*}{4L}\right)G^{-1}(\theta)\tan(\theta)[\cos\theta_T - \cos\theta]. \tag{50}$$

We could also have used the result of the dimensional analysis for the viscous dissipation (i.e. equation (21)) and this would result in $(3\tan\theta)/4L$ being replaced by $k\tan(\theta/2)$. When the dynamic contact angle, θ, is approaching the observed equilibrium contact angle, θ_T, we can re-write equation (50) using the variable $u = \theta - \theta_T$,

$$\left(\frac{\mathrm{d}u}{\mathrm{d}t}\right) = -\left(\frac{3v^*}{4L}\right)G^{-1}(\theta_T+u)\tan(\theta_T+u) \times [\cos\theta_T - \cos(u+\theta_T)] \tag{51}$$

which to first order in u is,

$$\left(\frac{\mathrm{d}u}{\mathrm{d}t}\right) \approx -\left(\frac{3v^*}{4L}\right)G^{-1}(\theta_T)\cos\theta_T. \tag{52}$$

This can be solved to give an exponential approach to equilibrium with,

$$\theta(t) \approx \theta_T + \exp[-(t+t_o)/\tau] \tag{53}$$

where t_o is a constant of integration and τ is a time constant given by,

$$\tau = \left(\frac{3v^*}{4L}\right)G^{-1}(\theta_T)\cos\theta_T = \left(\frac{3v^*}{4L}\right)\left(\frac{\pi}{3\Omega}\right)^{1/3} \times (2+\cos\theta_T)^{4/3}(1-\cos\theta_T)^{2/3}\cos\theta_T. \tag{54}$$

Assuming that the texture effect is a Wenzel roughness one (i.e. $\cos\theta_T = r_s\cos\theta_e$), this time constant will always decrease as roughness increases provided the Young's law contact angle, θ_e, is below around 48.3°. In this case, the approach to the equilibrium Wenzel contact angle will be faster due to the roughness than the approach to the Young's law contact angle would be on a flat and smooth surface. However, above the value $\theta_e = 48.3°$, equation (54) predicts that the time constant will initially increase as roughness increases before decreasing towards zero at larger levels of roughness.

5. Conclusions

In this work we have considered how topographic amplification of the affects of surface chemistry on static wetting also results in modification of dynamic wetting. In the case of a Wenzel rough surface with a Young's law contact angle less than 90° and a Cassie–Baxter composite solid–liquid surface the topography results in a large spreading power. This can result in droplets spreading more rapidly and, in

some cases, becoming completely spread even though they would only partially wet a flat and smooth surface of the same surface chemistry. We have discussed how the topography causes an increased out-of-balance surface tension force, which drives this increase in spreading rate. This effect has been summarized in simple terms by a modified Hoffman–de Gennes relationship between the edge speed and the dynamic and equilibrium contact angles. In the case of the complete spreading of small non-volatile droplets and stripes of liquid, simple power law changes of the geometric parameters are predicted. Whereas, in the case of partial wetting on surface, topography results in an exponential approach to equilibrium with a time constant dependent on the surface structure.

References

[1] de Gennes P G 1985 *Rev. Mod. Phys.* **57** 827
[2] Léger L and Joanny J F 1992 *Rep. Prog. Phys.* **55** 431
[3] Hoffman R L 1975 *J. Colloid Interface Sci.* **50** 228
[4] Kistler S H 1993 *Wettability* ed J C Berg (New York: Dekker) chapter 6, pp 311–429
[5] Voinov O V 1976 *Fluid Dyn.* **11** 714
[6] de Gennes P G 1984 *C. R. Acad. Sci.* II **298** 111
[7] Dussan E B and Davis S H 1974 *J. Fluid Mech.* **65** 71
[8] Cox R G 1986 *J. Fluid Mech.* **168** 169
[9] Hocking L M 1992 *J. Fluid Mech.* **239** 671
[10] Tanner L H 1979 *J. Phys. D: Appl. Phys.* **12** 1473
[11] McHale G, Rowan S M and Newton M I 1994 *J. Phys. D: Appl. Phys.* **27** 2619
[12] McHale G, Newton M I, Rowan S M and Banerjee M 1995 *J. Phys. D: Appl. Phys.* **28** 1925
[13] Abbott S 2008 *How To Be a Great Screen Printer: The Theory and Practice of Screen Printing* ed S Abbott, T Church, D Parker and A Harris (Oxford: MacDermid Autotype)
[14] Lopez J, Miller C A and Ruckenstein E 1976 *J. Colloid Interface Sci.* **56** 460
[15] Brochard-Wyart F, Hervet H, Redon C and Rondelez F 1991 *J. Colloid Interface Sci.* **142** 518
[16] Redon C, Brochard-Wyart F, Hervet H and Rondelez F 1992 *J. Colloid Interface Sci.* **149** 580
[17] Blake T D and Haynes J M 1969 *J. Colloid Interface Sci.* **30** 421
[18] Blake T D 1993 *Wettability* ed J C Berg (New York: Dekker) chapter 5, pp 251–308
[19] Blake T D 2006 *J. Colloid Interface Sci.* **299** 1
[20] Lipowsky R 2001 *Curr. Opin. Colloid Interface Sci.* **6** 40
[21] Darhuber A A and Troian S M 2005 *Annu. Rev. Fluid Mech.* **37** 425
[22] Barthlott W and Neinhuis C 1997 *Planta* **202** 1
[23] Onda T, Shibuichi S, Satoh N and Tsujii K 1996 *Langmuir* **12** 2125
[24] Roach P, Shirtcliffe N J and Newton M I 2008 *Soft Matter* **4** 224
[25] Cassie A B D and Baxter S 1944 *Trans. Faraday Soc.* **40** 546
[26] Bico J, Marzolin C and Quéré D 1999 *Europhys. Lett.* **47** 220
[27] Quéré D, Lafuma A and Bico J 2003 *Nanotechnology* **14** 1109
[28] Dupuis A and Yeomans J M 2005 *Langmuir* **21** 2624
[29] Kusumaatmaja H and Yeomans J M 2007 *Langmuir* **23** 6019
[30] Wenzel R N 1936 *Ind. Eng. Chem.* **28** 988
[31] Bico J, Tordeux C and Quéré D 2001 *Europhys. Lett.* **55** 214
[32] McHale G, Shirtcliffe N J and Newton M I 2004 *Analyst* **129** 284
[33] McHale G and Newton M I 2002 *Colloids Surf.* A **206** 193
[34] McHale G, Shirtcliffe N J, Aqil S, Perry C C and Newton M I 2004 *Phys. Rev. Lett.* **93** 036102
[35] Aqil S 2006 Wetting of microstructured surfaces *PhD Thesis* Nottingham Trent University
[36] McHale G 2007 *Langmuir* **23** 8200
[37] Bico J, Tordeux C and Quéré D 2001 *Europhys. Lett.* **55** 214
[38] Quéré D 2002 *Physica* A **313** 32
[39] Courbin L, Denieul E, Dressaire E, Roper M, Ajdari A and Stone H A 2007 *Nat. Mater.* **6** 661
[40] Bird R B, Stewart W E and Lightfoot E N 1960 *Transport Phenomena* (New York: Wiley)
[41] Ishino C, Reyssat M, Reyssat E, Okumura K and Quéré D 2007 *Europhys. Lett.* **79** 56005
[42] Hu C and Scriven L E 1971 *J. Colloid Interface Sci.* **35** 85
[43] Brochard-Wyart F and de Gennes P G 1994 *Langmuir* **10** 2440
[44] Brochard-Wyart F, de Gennes P G, Hervet H and Redon C 1994 *Langmuir* **10** 1566
[45] Ranabothu S R, Karnezis C and Dai L L 2005 *J. Colloid Interface Sci.* **288** 213
[46] de Ruijter M J, Blake T D and De Coninck J 1999 *Langmuir* **15** 7836
[47] Petrov J G, Ralston J and Hayes R A 1999 *Langmuir* **15** 3365
[48] Ellis J S, McHale G, Hayward G L and Thompson M 2003 *J. Appl. Phys.* **94** 6201